Drug Design, Development and Therapy

Dovepress
Taylor & Francis Group

Open Access Full Text Article

ORIGINAL RESEARCH

Multi-Target Mechanism of Compound Qingdai Capsule for Treatment of Psoriasis: Multi-Omics Analysis and Experimental Verification

Yuanyuan Qiao[1,2], Canzhe Li[1], Chupeng Chen[1], Peilin Wu[1], Yibing Yang[1], Mingxiang Xie[1,3], Na Liu[1], Jiangyong Gu[1]

[1]Research Centre of Basic Integrative Medicine, School of Basic Medical Sciences, Guangzhou University of Chinese Medicine, Guangzhou, 510006, People's Republic of China; [2]The First Affiliated Hospital of Guangzhou University of Chinese Medicine, Guangdong Clinical Research Academy of Chinese Medicine, Guangzhou, 510405, People's Republic of China; [3]The Fifth Affiliated Hospital, Southern Medical University, Guangzhou, Guangdong, 510910, People's Republic of China

Correspondence: Jiangyong Gu, Research Centre of Basic Integrative Medicine, School of Basic Medical Sciences, Guangzhou University of Chinese Medicine, Guangzhou, 510006, People's Republic of China, Tel +020-39358909, Email gujy@gzucm.edu.cn

Drug Design, Development and Therapy downloaded from https://www.dovepress.com/
For personal use only.

Background: Psoriasis is a chronic skin disease affected by genetic and autoimmunity. The traditional Chinese medicine, Compound Qingdai Capsule (CQC), has shown potential benefits in treating psoriasis in clinical settings. Despite its efficacy, the molecular mechanisms underpinning its therapeutic action remain unclear.

Purpose: This study aimed to unravel the molecular mechanism of Compound Qingdai Capsule for psoriasis based on the psoriasis pathogenic pathway network, integrating multi-omics analysis, systems pharmacology, machine learning modeling, and animal experimentation.

Methods: Psoriasis pathogenic pathway network was constructed through employing bioinformatics analysis and psoriasis-related multi-omics data mining. The ingredients of CQC were detected by UPLC-MS/MS, and target prediction was performed by systems pharmacology. Machine learning, including Lasso regression, Random Forest, and Support Vector Machine (SVM), were utilized to screen core targets of psoriasis. Molecular docking was employed to evaluate the binding affinity between ingredients and core targets. The expression levels of core targets were determined using qRT-PCR and ELISA.

Results: Psoriasis-related datasets GSE201827 and GSE174763 were comprehensively analyzed to obtain 635 psoriasis-related genes. These genes were further enriched to elucidate signaling pathways involved, leading to the construction of psoriasis pathogenic pathway network. Utilizing UPLC-MS/MS, 29 main ingredients of CQC were characterized. CQC ingredients-targets network was constructed using these ingredients and their targets. Screening of CQC anti-psoriasis core targets using machine learning algorithm. Molecular docking confirmed good binding affinity between these targets and ingredients. Imiquimod (IMQ) induced psoriasis-like rat validated the anti-psoriasis effect of CQC by alleviating symptoms, reducing spleen and thymus index, and modulating the expressions of core targets at mRNA and protein levels.

Conclusion: CQC effectively modulates the expression levels of AURKB, CCNB1, CCNB2, CCNE1, CDK1, and JAK3 through various ingredients, such as astilbin, salvianolic acid A, and engeletin, via multiple pathways, thereby alleviating psoriasis-like symptoms.

Keywords: systemic pharmacology, machine learning, compound qingdai capsule, psoriasis, molecular mechanism

Introduction

Psoriasis is a chronic, inflammatory disorder with genetic and autoimmune traits. It is characterized by pimples, erythema, and silvery-white scaled lesions, limiting to certain areas or wide-spreading on the body.[1] Psoriasis affects about 2–3% of the global population,[2] and they are more likely than the normal population to suffer from systemic diseases such as diabetes mellitus, hypertension, myocardial infarction, chronic obstructive pulmonary disease, metabolic syndrome,[3] among others, and the prevalence of concomitant psychiatric disorders, such as depression, anxiety and

Received: 20 February 2025
Accepted: 10 June 2025
Published: 18 June 2025

© 2025 Qiao et al. This work is published and licensed by Dove Medical Press Limited. The full terms of this license are available at https://www.dovepress.com/terms.php and incorporate the Creative Commons Attribution – Non Commercial (unported, v4.0) License (http://creativecommons.org/licenses/by-nc/4.0/). By accessing the work you hereby accept the Terms. Non-commercial uses of the work are permitted without any further permission from Dove Medical Press Limited, provided the work is properly attributed. For permission for commercial use of this work, please see paragraphs 4.2 and 5 of our Terms (https://www.dovepress.com/terms.php).

Graphical Abstract

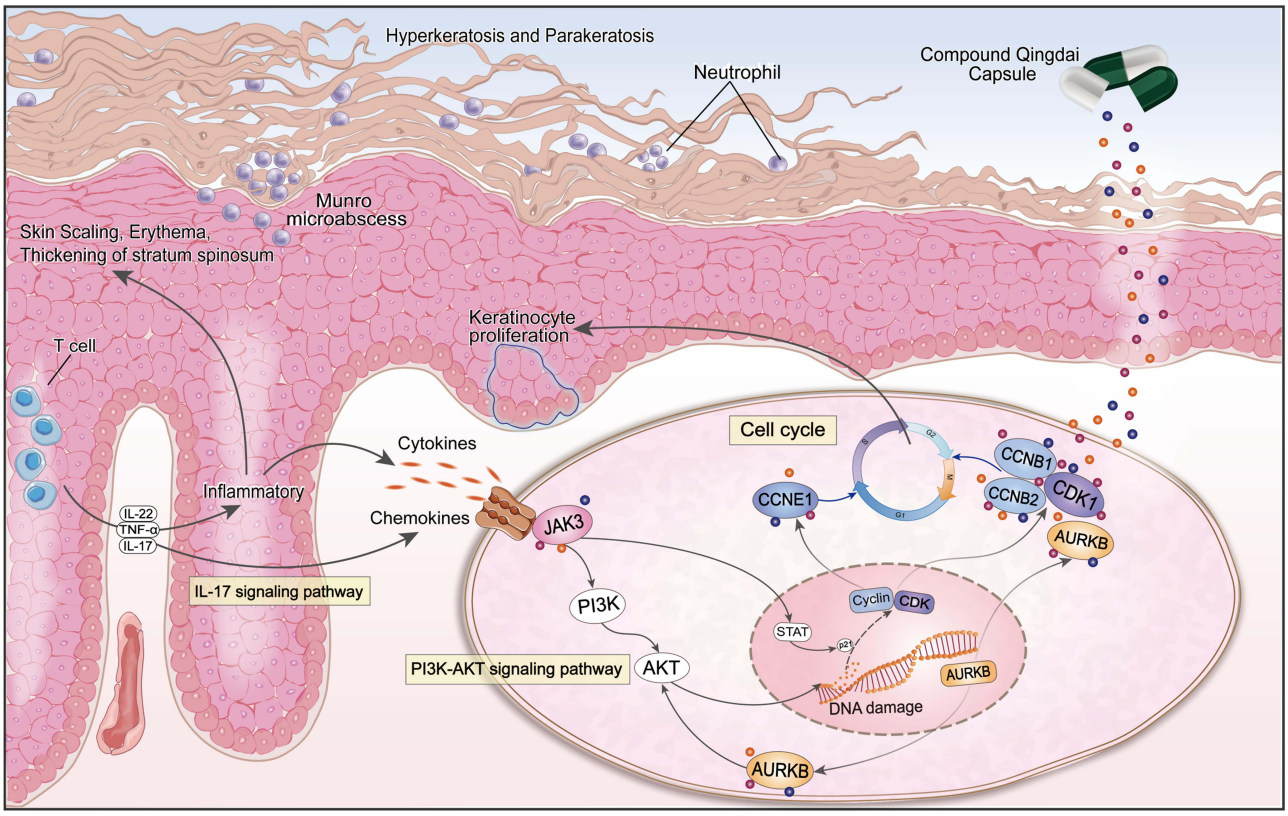

suicidal thoughts, has been escalating annually.[4] The condition in question engenders considerable distress for affected individuals and concurrently contributes to societal burden.

At present, the etiology and pathogenesis of psoriasis remain completely clarified, and modern medicine recognizes that psoriasis is affected by a variety of factors such as genetic, environment, immunity, inflammation, and other variables.[5] Intrinsic immunity mediated by keratinocytes, dendritic cells and neutrophils, and adaptive immunity mediated by T cells serve as the initiation and pivotal aspects of psoriasis pathogenesis. The interaction of inflammatory factors and chemokines during these processes can trigger and worsen psoriasis symptoms.[6,7] Therefore, in accordance with the principles of anti-inflammatory action, anti-proliferative, and regulation of epidermal cell differentiation, current therapeutic strategies include topical treatments, phototherapy, immunomodulatory agents, and biologic medications. The objective of these strategies is to alleviate symptoms and enhance the overall quality of life. However, obstacles including adverse effects, medication resistance, elevated expenses, and variability in patient reactions constrain the effectiveness of these treatments.[8] Consequently, the development of more efficacious and secure treatment protocols holds paramount importance.

Against this background, as precious gemstone in the realm of traditional medicine, Traditional Chinese Medicine (TCM) shows unique advantages in the treatment of psoriasis. Among them, Compound Qingdai Capsule (CQC), as a typical Chinese patent medicine formula, has achieved remarkable efficacy in the treatment of psoriasis. CQC is a traditional herbal formula with the effects of clearing heat and removing toxins, resolving blood stasis and eliminating blemishes, dispelling wind and relieving itching. Its essence may be consistent with CQC's anti-inflammatory effect, inhibition of keratinocyte proliferation and anti-angiogenesis. Studies have shown that CQC can reduce the levels of

psoriasis-related inflammatory factors such as IL-2, IL-8, IL-18, and IFN-γ.[9] It can down regulated the content of secretory factors of Th1 cells and up regulated that of Th2 cells, thus improving the skin lesions of patients with advanced psoriasis vulgaris.[10] CQC contains a variety of herbs, including *Indigo Naturalis*. (Qingdai), *Portulaca Oleracea*. (Machixian), *Radix Angelicae Dahuricae*. (Baizhi), *Rhizoma Smilacis Glabrae*. (Tufuling), *Radix Lithospermi*. (Zicao), *Cyrtomium Fortunei*. (Guanzhong), *Taraxacum Mongolicum*. (Pugongying), *Salvia Miltiorrhiza*. (Danshen), *Rhizoma Dioscoreae Hypoglaucae*. (Fenbixie), *Cortex Dictamni*. (Baixianpi), *Fructus Mume*. (Wumei), *Kadsura Longipedunculata*. (Nanwuweizi), *Crataegus Pinnatifida*. (Shanzha) and *Massa Medicata Fermentata*. (Jianqu). It was traditionally used to treat acute flushing, rash, and desquamative dermatoses, especially psoriasis. After development and improvement, it has become a commercially available medicinal product (registration number Z20010157) approved by medical authorities, and the "Guideline for the diagnosis and treatment of psoriasis in China (2023 edition)" officially recommends CQC for psoriasis management.[11] While the CQC has demonstrated a certain level of effectiveness in treating psoriasis,[12] the underlying mechanism of its action remains incompletely understood.

Recently, multi-omics technology has become popular in psoriasis research to rapidly and comprehensively discover the pathogenesis of psoriasis as well as biomarkers associated with psoriasis drugs.[13] The multi-omics analytical strategy is expected to accelerate the uncovering of TCM in the treatment of diseases.[14] Machine learning serves as a crucial instrument for multi-omics research by facilitating intelligent data processing, analyzing different features of biological data, and integrating all the features to form a predictive mode. Machine learning has extensive applications in the analysis of multi-omics data, enabling disease subtype classification, biomarker discovery, and pathway analysis.[15–17] Algorithms like Lasso regression, SVM, and Random Forest are commonly used.[18] The integration of multi-omics data analysis and machine learning modeling offers novel research directions for exploring the pathogenesis and therapeutic mechanisms underlying psoriasis.

In this study, Gene Expression Omnibus (GEO) database was utilized to mine psoriasis-related datasets for target genes. These genes were subjected to KEGG enrichment analysis to construct psoriasis pathogenic pathway network. The main ingredients of CQC were detected by UPLC-MS/MS, and CQC ingredients-targets network was constructed using systems pharmacology. Based on GSE201827 dataset, Lasso regression, Random Forest and SVM models were constructed to identify core targets, which were validated using ROC curves and molecular docking. The workflow of the above analysis is shown in Figure 1. IMQ induced psoriasis-like rats were introduced to evaluate the anti-psoriasis efficacy of CQC in multidimensional manners. The qRT-PCR and ELISA were employed to detect the changes in expression of core targets.

Materials and Methods

Dataset Collection and Analysis

The psoriasis-related datasets, GSE201827 and GSE174763, were obtained from GEO database (https://www.ncbi.nlm.nih.gov/geo/), which encompassed both non-lesional skin (NL) and lesional skin (LS) samples collected from patients diagnosed with psoriasis vulgaris.[19,20] GSE201827 is an array expression dataset containing 70 NL samples and 63 LS samples, and GSE174763 is a miRNA dataset containing 69 NL samples and 67 LS samples. The data were subjected to preprocessing utilizing the R software (version 4.2.1; https://www.r-project.org/). Principal component analysis (PCA) was conducted on the sample data from both NL and LS groups, employing the FactoMineR package. Furthermore, normalization was achieved through the application of the rma function within the affy package. DEGs and DEMs were identified by applying the limma package with the statistical standard of "$P < 0.05$" and "$|\log2 \text{ Fold Change}| > 1$". To retrieve validated DEMs-related genes, the MultiMiR package was employed. The overlapping genes between DEMs and DEGs were taken as psoriasis-related targets.

Network Construction of Psoriasis Pathogenic Pathways

The KEGG enrichment analysis of psoriasis-related target genes was analyzed within the clusterProfiler package, with the species defined as "Homo sapiens" and the parameters set to "pvalue < 0.05" and "qvalue < 0.05". And the visualization of top 20 pathways, sorted by gene counts, were accomplished using the ggplot2 package. By examining

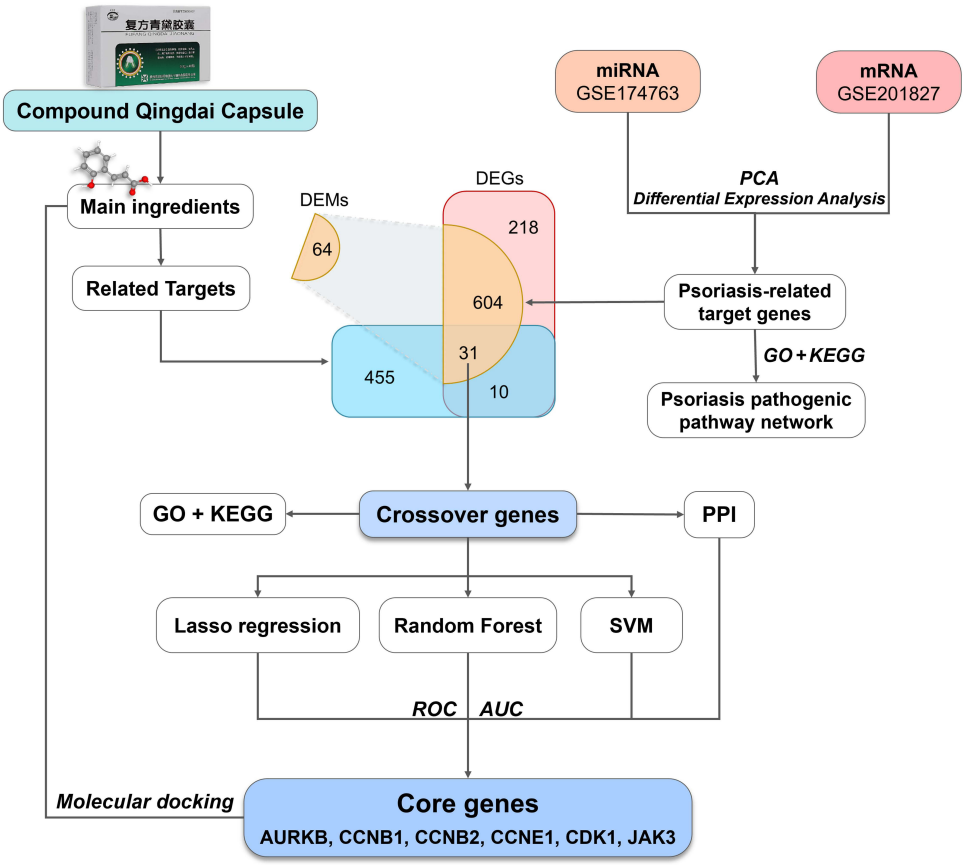

Figure 1 Multi-Omics and systems pharmacology analysis workflow on CQC anti-psoriasis core targets.

the KEGG database (https://www.genome.jp/kegg/) and reviewing existing literature, these pathways and psoriasis-related target genes were consolidated to construct a psoriasis pathogenic pathway network.

Identification of the Chemical Constitution of CQC

The CQC powder (20 mg) was weighed and mixed thoroughly with 500 μL of methanol using ultrasonication (40 hz, 300 W), then centrifuged at 13,000 rpm for 10 min, and the supernatant was taken as sample. The samples were analyzed using the UltiMate 3000 UHPLC system with C18 column (1.9 μm, 2.1×100 mm), the flow rate was 0.3 mL/min, and the injection volume was 10 μL, and the mobile phase was 0.1% formic acid/acetonitrile-0.1% formic acid/water. The analysis was performed using data-dependent scanning analysis, with the loop count set to 10, and the HCD energy was stepwise normalized to the collision energy. And the chemical composition was compared using Compound discover software (V 3.2, Thermo Fisher Scientific, CA, USA). A semi-quantitative approximation of the relative proportions of compounds was achieved by calculating the "percent peak area" as the ratio of compound peak area to total peak area. After eliminating the intermediate compounds, the chemical components with peak area percentages greater than 0.1% were selected as the main ingredients of CQC.

Collection of Potential Targets for CQC Main Ingredients

The Super-PRED database[21] and the PubChem database (https://pubchem.ncbi.nlm.nih.gov/) were used to gather known targets of CQC main ingredients. Additionally, the predicted targets of CQC main ingredients were collected using the SwissTargetPrediction database (http://www.swisstargetprediction.ch/). Cytoscape software (version 3.7.2; https://cytoscape.org/) was utilized to construct the CQC ingredients-targets network and visualize ingredients-targets interactions.

Candidate Targets of CQC Anti-Psoriasis and Function Analysis

Crossover genes among DEMs-related genes, DEGs and CQC-related targets were taken as candidate targets of CQC anti-psoriasis. To explore the interaction among candidate target genes, these genes were submitted to the String database (https://cn.string-db.org/) to acquire information regarding the interrelationships among them. Subsequently, this interaction data was graphically represented as a Protein-Protein Interaction (PPI) network utilizing Cytoscape software, then the network was topologically analyzed with the cytoHubba plugin. The top 15 targets were identified as hub-genes by comprehensively ranking the candidate targets in terms of "Maximal Clique Centrality (MCC) Score" and "Degree". GO and KEGG enrichment analysis of CQC anti-psoriasis candidate targets was performed using the same methods described in previous. These enrichment results were comprehensively sorted by gene counts and pvalue, visualized using the GOplot package.

Integrating Multiple Machine Learning Algorithms to Identify CQC Anti-Psoriasis Core Targets

The gene expression matrix of candidate targets was extracted from GSE201827 dataset. All samples were randomly partitioned into training set, comprising 70%, and test set, comprising 30%, with sample grouping (NL and LS) as the ending variables and candidate targets as the input variables. The training set was used to construct machine learning models, and the test set was employed to assess the prediction accuracy of the machine learning algorithm. We use three algorithms, namely Lasso regression, Random Forest, and SVM, to screen featured genes through modeling by taking advantage of their strengths in analyzing high-dimensional datasets and identifying key targets. Lasso regression performs variable selection and regularization, simplifying models by shrinking less important coefficients to zero.[22] Random Forest combines multiple decision trees to improve prediction accuracy and provides feature importance scores, aiding in identifying critical molecular markers.[23] SVM handles non-linear relationships by mapping input data into high-dimensional space using kernel functions and generalizes well to unseen data.[24]

Lasso regression model was employed by the glmnet package, firstly inputting the training set to build the initial model, then selecting the lambda with the smallest average error (lambda.min) by 10-fold cross-validation approach, constructing the optimal model, inputting the test set into this model for prediction. Finally, the pROC software package facilitated model evaluation by generating receiver operating characteristic curves (ROCs) and calculating the area under the curve (AUC). In RF, the model was constructed using the RandomForest package, 500 decision trees were generated by default. The number of decision trees corresponding to the minimum error was derived by iterative calculation. And the best model was reconstructed, evaluated through ROC curve and AUC. Then the importance of candidate targets to the model was calculated by Mean Decrease Gini, and the top 15 targets were selected as important targets. SVM was performed by R package e1071. Four kernel functions, Linear Kernel, Polynomial Kernel, Radial Basis Kernel and Sigmoid Kernel, were set to construct the SVM model, and evaluated through ROC curve and AUC. These results were compared to select the kernel function with the highest prediction accuracy to build the best model and derive the feature targets.

Afterwards, the genes were taken as core targets for subsequent analysis within the intersection of feature targets obtained from three machine learning algorithms and the hub-genes of PPI. To verify the importance of core targets in the GSE201827 dataset, ROC curve and AUC were used to analyze the discrimination ability of core targets in the dataset, while *t*-test was deployed to statistically compare the expression levels of core targets between NL and LS groups.

Molecular Docking

The binding affinity of CQC main ingredients towards the core targets was calculated by molecular docking. The three-dimensional structures of main ingredients were retrieved from PubChem database, followed by the minimization of molecular energies utilizing Chem3D software (version 17.1). The protein structures of the core targets were downloaded from the RSCB PDB database; however, in cases where retrieval was unsuccessful, reliable predicted structures were obtained from the AlphaFold database.[25] Subsequently, the proteins underwent preprocessing utilizing PyMOL software (version 2.6; https://pymol.org/). Autodock 4.2.6 software was utilized to perform molecular docking of CQC main

ingredients with core target proteins to assess binding affinity. The protein-ligand complex conformation was imported into PyMOL and Discovery Studio softwares for visualization.

Reagents and Animal

IMQ cream was obtained from Sichuan Med-Shine Pharmaceutical Co., Ltd. (5%; Mingxinlidi, Chengdu, China). Methotrexate tables (MTX) were obtained from SPH Sine Pharmaceutical Laboratories Co., Ltd (Shanghai, China). Compound Qingdai Capsules was purchased from Tianning Pharmaceutical Co (Shaanxi, China). According to the recommended clinical dosage and the standard conversion factor for dosage equivalence between humans and rats, the MTX equivalent dose was 0.525 mg/kg, while the CQC equivalent dose was 0.63 g/kg, both prepared with distilled water.

SPF male SD rats (120–150 g) were purchased from Guangzhou Ruige Biotechnology Co. (SCXK[GD]2023–0059) and were housed in SPF Animal Experiment Center of Research Center of Integrative Medicine, Guangzhou University of Chinese Medicine, China (SYXK[GD]2023–0182). The environmental temperature was 20–25 °C under 12/12 h light/dark cycle. The humidity was 40–60%. The medical ethics committee approval was obtained from Guangzhou University of Chinese Medicine (Approval Number: 202207006008).

Animal Experiment

According to the ARRIVE 2.0 guidelines, the number of rat groups was set as 6, the effect size f was 0.25, the significance level was 0.05, the statistical power was 0.8, and the total sample size n was calculated to be 36, with 6 rats in each group, which also adhere to the 3Rs principle. All animals were acclimatized for 7 days, and then randomly allocated into 6 groups (n=6, per group): the control group (Con), the model group (IMQ), the positive control group (MTX, 0.525 g/kg), the CQC low dose group (CQC_L, 0.315 g/kg), the CQC medium dose group (CQC_M, 0.63 g/kg), and the CQC high dose group (CQC_H, 1.26 g/kg).

One day prior to the commencement of the experiment, the dorsal skin of rats was depilated to 2×3 cm. Five of six groups received IMQ cream (100 mg/day) to induce psoriasis-like model except for the blank group, where received petroleum jelly cream. This continued for 7 days. Following, MTX, serving as a positive control drug, was administered to the rats, and different dosages of CQC were administered to intervene in the psoriasis-like rat model. The Con and IMQ groups received equivalent dosages of distilled water. Administration was done by gavage at 1 mL/100 g body weight once daily for 7 days. This experimental design, consisting of a 7-day IMQ induction period followed by a 7-day drug intervention period, is based on well-established protocols in the literature.[26,27]

Psoriasis Area Severity Index (PASI) Assessment and Hematoxylin-Eosin (HE) Staining

To accurately assess the severity of psoriasis lesions in rats, the PASI scoring system was implemented daily on the dorsal skin of the experimental animals. The scoring system assigned numerical values ranging from 0 to 4 (0 represents none, 1 represents mild, 2 represents moderate, 3 represents pronounced, and 4 represents very pronounced), for each of the three parameters: scaling, erythema, and infiltration. The total PASI score for per animal ranged from 0 to 12, providing a comprehensive evaluation of the psoriatic lesions. Upon completion of the animal experiment, the rats were euthanized. Their dorsal skins were excised and bisected, with one half being stored at −80 °C for further analysis, and the other half was preserved in formalin for next paraffin embedding, sectioning and HE staining for histopathological analysis.

Spleen Index and Thymic Index

The initial step involved recording the weights of the rats. Following the euthanasia procedure, the spleen and thymus of the rats were promptly excised in their entirety and accurately measured. Subsequently, the spleen index and thymus index were derived by dividing the respective organ weights by the body weight of the rats.

qRT-PCR

The total RNA of rat skin tissues was extracted in accordance with the instructions of Trizol Reagent kit (Solarbio, R1200, Shanghai, China), and being utilized as a template in cDNA reverse transcription synthesis manufactured by

Table 1 Primers Used in qRT-PCR

Target Gene	Forward Primer (5′-3′)	Reverse Primer (5′-3′)
Actb	AGCCATGTACGTAGCCATCC	ACCCTCATAGATGGGCACAG
Aurkb	GGTCCAACAGCCAGTCCACAG	ACGCCCAATCTCAAAGTTGTCAATG
Ccnb1	TCCCACACGGAGGAATCTCT	TCTGCAGACGAGGTAGTCCA
Ccnb2	CGACTACGACATGGTGCATTAC	TCTTGACAGCGATGAACTTGGT
Ccne1	CCTGCTCACTGCTCTGCTTCTTAC	CAACATCCAGACCCACACCAACAG
Cdk1	CGGTTGACATCTGGAGCATA	GCATTTTCGAGAGCAAGTCC

a two-step Kit with gDNA Clean (Accurate Biotechnology, AG11728, Hunan, China). Real-time fluorescence quantitative PCR was performed using SYBR Green Premix (Accurate Biotechnology, AG11701, Hunan, China) by Bio-rad CFX96 Quan-titative PCR device. The expression levels of all genes were compared with ACTB, and the primer sequences were shown in Table 1. The results were analyzed by the $2^{-\Delta\Delta ct}$ method.

Elisa

Protein samples were extracted from rat skin tissues by the techniques of cryogenic milling after addition of phosphate buffered saline to the tissues. Subsequently, total protein levels of the samples were assayed using BCA method, and the levels of core target proteins in the samples were determined by employing ELISA kits by sandwich-assay (Bioswamp, Wuhan, China), following the manufacturer's protocol. The results were derived by calculating the ratio of the core target protein level to the total protein level.

Statistical Analysis

In this study, all data were expressed as the mean ± SD or the mean ± SEM. The plotting and statistical analysis were conducted utilizing R software. The one-way ANOVA test was employed to compare the groups. When variances were homogeneous, pairwise comparisons between groups were conducted using the Least Significant Difference (LSD) method. When variances were not equal, Dunnett's T3 test was used. A p-value of less than 0.05 was considered to indicate statistical significance.

Results

Analysis of Psoriasis-Associated DEGs and DEMs to Construct Psoriasis Pathogenic Pathway Network

GSE201827 and GSE174763 datasets underwent data preprocessing to exclude outlier anomalous samples from both the NL and LS groups. Upon conducting PCA, the resulting scatter plots (Figure 2A and C) revealed distinct clustering patterns among most samples within both the NL and LS groups. This indicated good reproducibility of samples within each group and high similarity of the data. Furthermore, the samples exhibited comparability between the two groups. Subsequently, normalization was performed on the datasets to eliminate inter-chip variations, ensuring that the expression data across all chips were comparable for further analysis.

Using limma package, differential analysis of the sample between NL and LS group from GSE201827 yielded 863 DEGs, containing 492 up-regulated genes and 371 down-regulated genes (Figure 2B); and differential analysis of the GSE174763 dataset yielded 66 DEMs, containing 33 up-regulated miRNAs and 33 down-regulated miRNAs (Figure 2D). Subsequently, the MultiMiR package was utilized to retrieve 747 validated genes that correspond to the identified 66 DEMs. Finally, 635 crossover genes were identified between the DEMs-related genes and the DEGs and designated as psoriasis-related target genes.

Figure 2E exhibits the KEGG pathway enrichment results pertaining to psoriasis-related target genes. The distribution of psoriasis-related genes across these signaling pathways was explored within the KEGG database, enabling the construction of psoriasis pathogenic pathway network (Figure 2F).

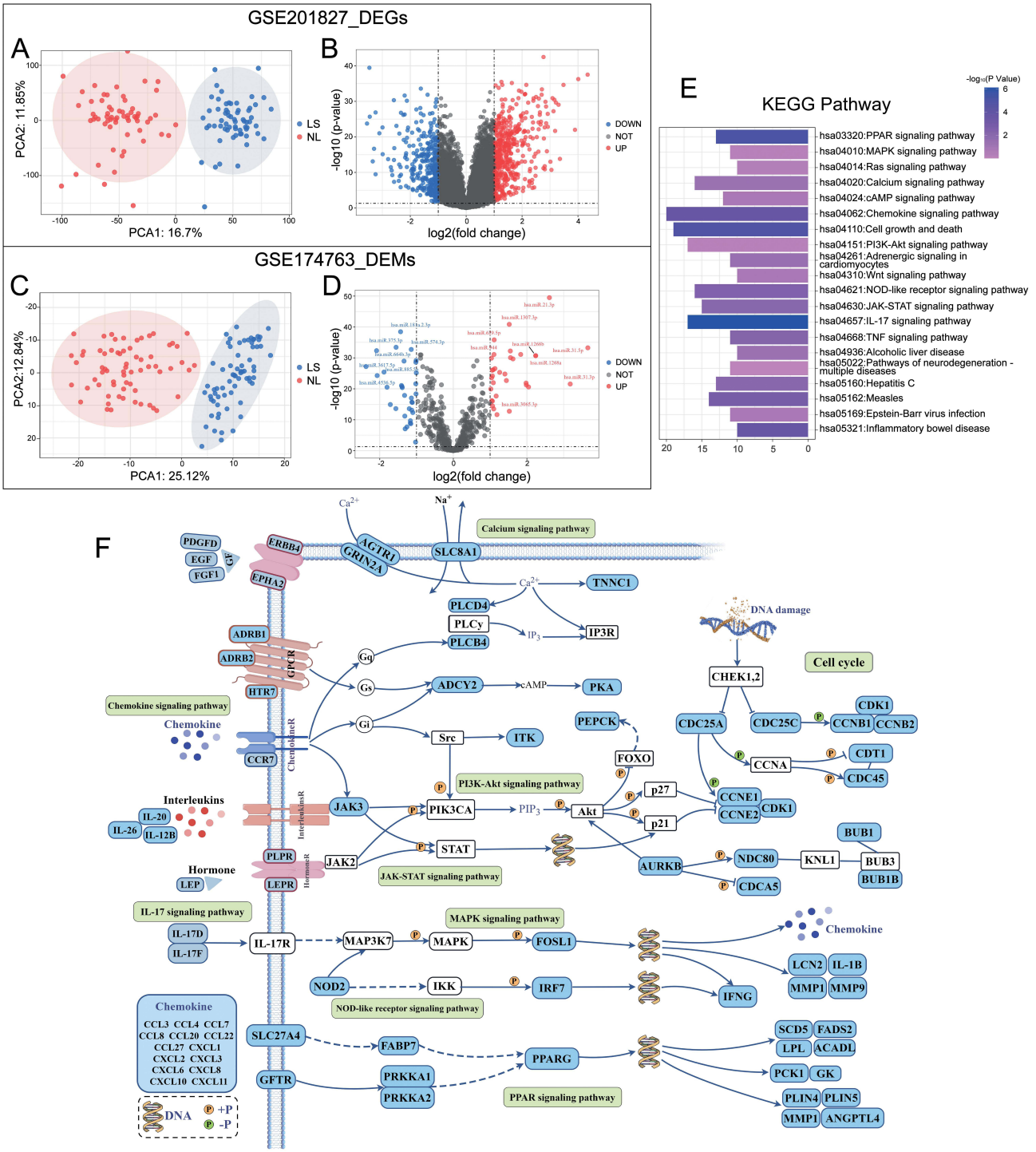

Figure 2 Acquisition of psoriasis-associated DEGs and DEMs and construction of the psoriasis pathogenic pathway network. (**A**) PCA plot showed sample distribution for both NL and LS groups in the GSE201827 dataset; (**B**) Volcano plot showed all differentially expressed genes screened from GSE201827 dataset. (**C**) PCA plot showed sample distribution for both NL and LS groups in the GSE174763 dataset; (**D**) Volcano plot showed all differentially expressed miRNAs screened from GSE174763 dataset. (**E**) KEGG pathway of psoriasis-related genes. (**F**) Network diagram of psoriasis pathogenic pathways.

Main Ingredients and Targets of CQC

The chemical fingerprinting analysis of CQC revealed the identification of 199 distinct chemical components. These components are enumerated in Figure 3A and B, arranged in the order of their retention times. And 29 CQC main ingredients were obtained after "percentage of peak area" screening (Table 2), including caffeic acid, astilbin, rosmarinic

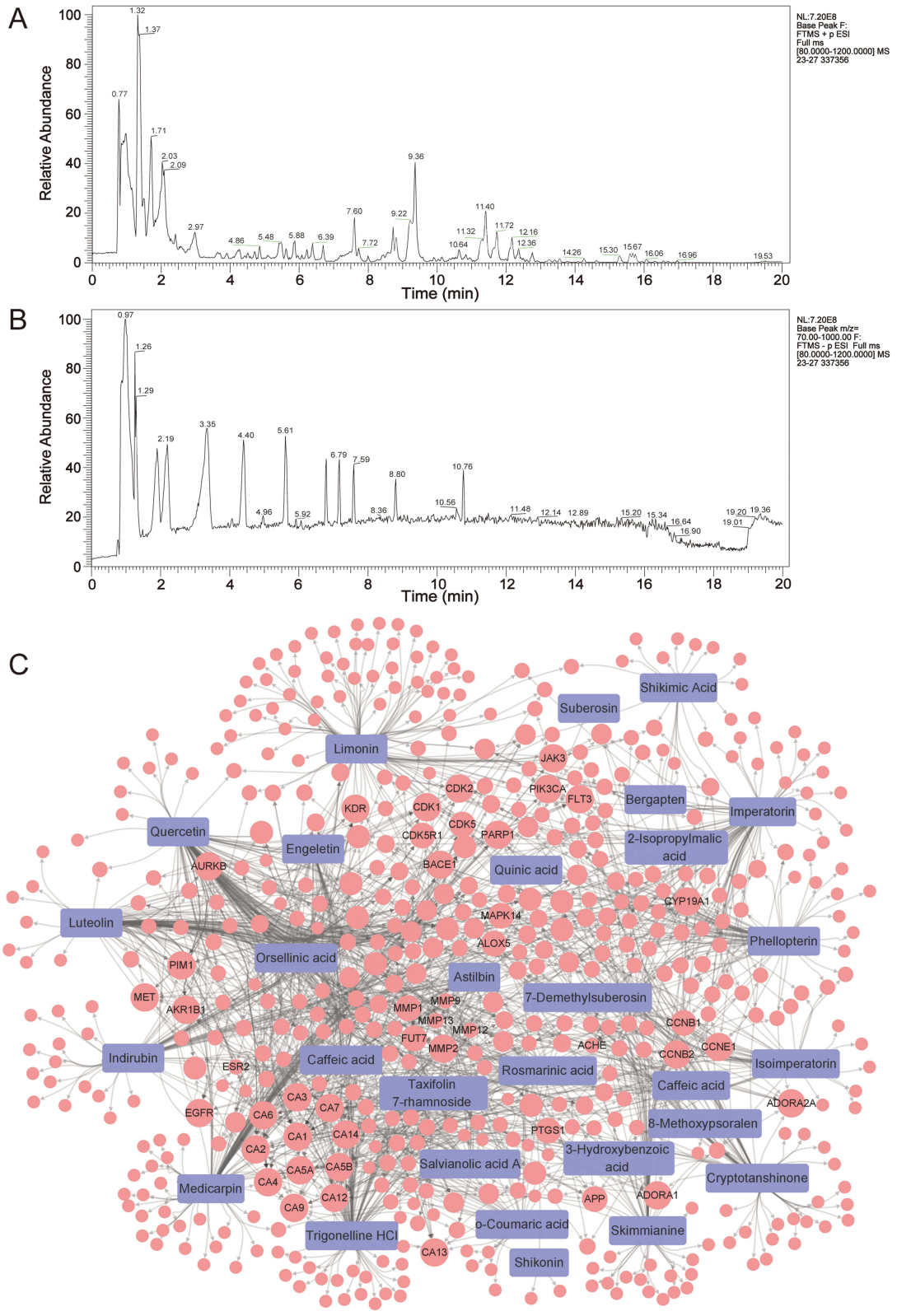

Figure 3 Compositional analysis of CQC and obtaining their predicted targets. (**A** and **B**) Base peak chromatogram of Compound Qingdai Capsules in positive (**A**) and negative (**B**) ion modes. (**C**) Ingredients-Targets Network Diagram of CQC. Purple squares are main ingredients, red circles are targets.

https://doi.org/10.2147/DDDT.S523836

Table 2 Main Ingredients of Compound Qingdai Capsule

Compound Name	Formula	Mass	RT (min)	Percentage of Peak area (%)	PubChem CID
Caffeic acid	$C_9H_8O_4$	180.04223	4.392	4.197709	689043
Quinic acid	$C_7H_{12}O_6$	192.06324	1.010	3.156601	6508
Astilbin	$C_{21}H_{22}O_{11}$	450.11581	5.920	3.11053	119258
o-Coumaric acid	$C_9H_8O_3$	164.04721	5.634	2.83871	637540
Medicarpin	$C_{16}H_{14}O_4$	270.08898	10.758	1.846029	336327
Imperatorin	$C_{16}H_{14}O_4$	270.08857	11.403	1.177336	10212
Limonin	$C_{26}H_{30}O_8$	516.19886	9.726	1.13028	179651
8-Methoxypsoralen	$C_{12}H_8O_4$	216.04196	8.677	1.040874	4114
7-Demethylsuberosin	$C_{14}H_{14}O_3$	230.09402	10.564	0.952954	5316525
Salvianolic acid A	$C_{26}H_{22}O_{10}$	494.12075	7.297	0.846125	5281793
Engeletin	$C_{21}H_{22}O_{10}$	434.12083	6.529	0.709032	6453452
Phellopterin	$C_{17}H_{16}O_5$	300.09908	11.727	0.623016	98608
Rosmarinic acid	$C_{18}H_{16}O_8$	360.08432	6.701	0.579498	5281792
Trigonelline HCl	$C_7H_7NO_2$	137.04763	5.470	0.558135	5571
Isoimperatorin	$C_{16}H_{14}O_4$	270.08858	12.166	0.553465	68081
2-Isopropylmalic acid	$C_7H_{12}O_5$	176.0683	3.449	0.541564	77
Gallic acid	$C_7H_6O_5$	170.02135	1.370	0.530182	370
Shikimic Acid	$C_7H_{10}O_5$	174.05258	1.074	0.430629	8742
Orsellinic acid	$C_8H_8O_4$	168.04207	1.765	0.387204	68072
3-Hydroxybenzoic acid	C_5H_5NO	95.03711	1.054	0.356262	7420
Quercetin	$C_{15}H_{10}O_7$	302.04249	7.628	0.277717	5280343
Luteolin	$C_{15}H_{10}O_6$	286.04762	7.619	0.275128	5280445
Suberosin	$C_{15}H_{16}O_3$	244.10946	12.361	0.232777	68486
Cryptotanshinone	$C_{19}H_{20}O_3$	296.14065	12.757	0.197771	160254
Bergapten	$C_{12}H_8O_4$	216.04196	9.255	0.187548	2355
Skimmianine	$C_{14}H_{13}NO_4$	259.08406	8.428	0.17593	6760
Taxifolin 7-rhamnoside	$C_{21}H_{22}O_{11}$	450.11556	6.078	0.149586	5070785
Indirubin	$C_{16}H_{10}N_2O_2$	262.07372	10.939	0.133529	10177
Shikonin	$C_{16}H_{16}O_5$	270.08858	10.473	0.114666	479503

acid, salvianolic A, engeletin, and others. Subsequently, 49 known targets and 483 predicted targets associated with the main ingredients of CQC were assembled through multiple database searches, a total of 496 CQC-related targets were obtained after removing duplicates. The ingredients-Targets Network of CQC is shown in Figure 3C, containing 525 nodes and 1323 edges.

PPI and Enrichment Analysis of CQC Anti-Psoriasis Candidate Targets

The Venn diagram (Figure 4A) showed 31 crossover genes among DEMs-related genes, DEGs, and CQC-related targets, which were taken as candidate targets of CQC anti-psoriasis. These candidate targets were then loaded into the STRING database generate PPI networks and topologically analyzed by the cytohubba plug-in of Cytoscape, and hub-genes were identified based on the top 15 rankings derived from a combined assessment of "MCC Score" and "Degree" (Figure 4B).

GO enrichment analysis (Figure 4C) of the candidate targets revealed that the anti-psoriasis effects of CQC primarily concentrate on nuclear chromosome segregation, the regulation of cyclin-dependent protein kinase activity and various other biological processes, and cyclin-dependent protein kinase holoenzyme complex, protein kinase complex and other cellular components, and several molecular functions such as cyclin-dependent protein serine/threonine kinase regulator activity and kinase regulator activity. In addition, KEGG analysis demonstrated those candidate targets of CQC anti-

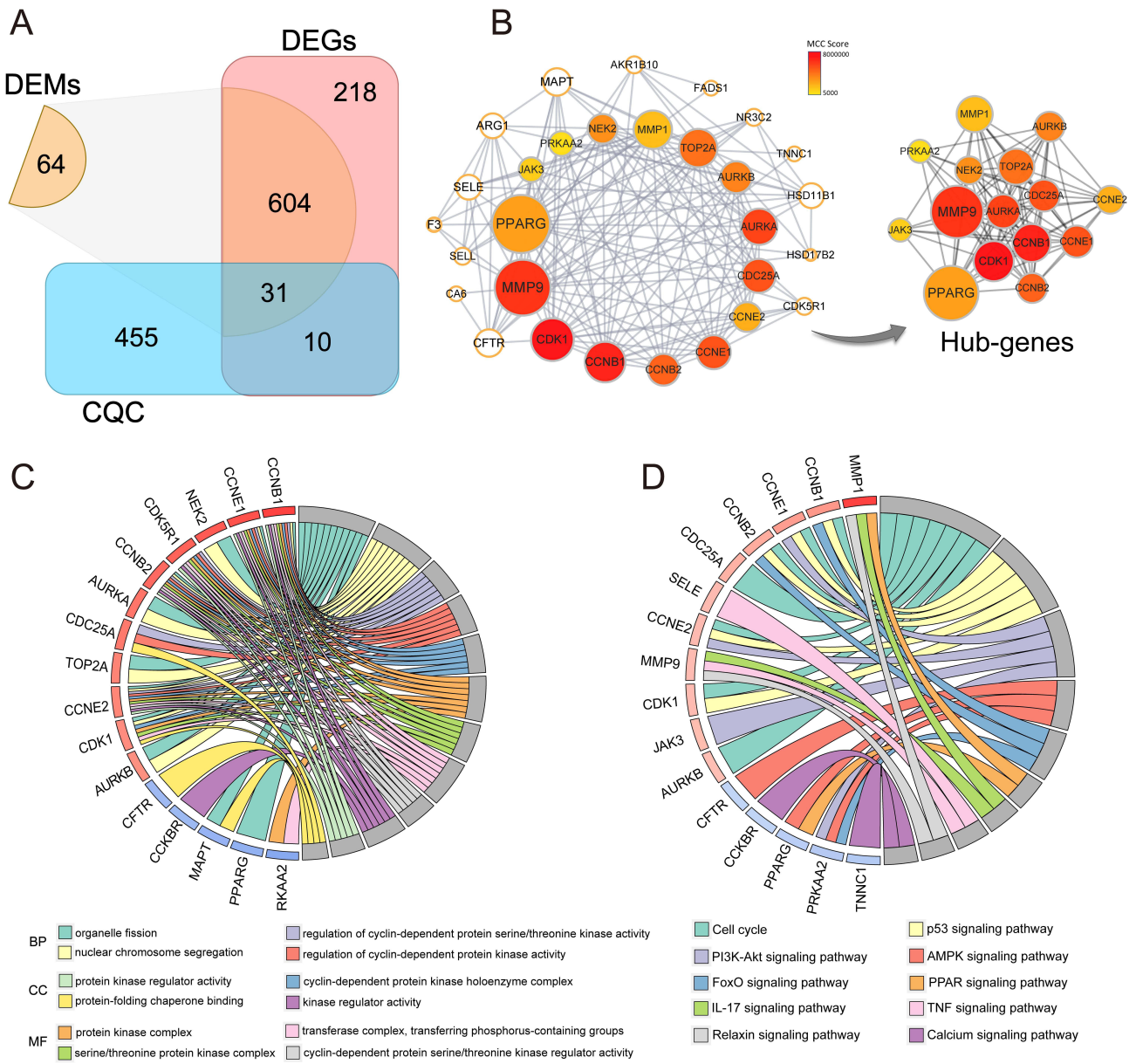

Figure 4 Candidate targets of CQC anti-psoriasis, and PPI, GO and KEGG pathway enrichment. (**A**) Venn diagram showed crossover genes (CQC anti-psoriasis candidate targets) among DEMs-related genes, DEGs and CQC-related targets. (**B**) PPI network diagram of CQC anti-psoriasis candidate targets, and Hub-genes analyzed by cytoHubba. Node color is correlated with MCC score. The size of the node is positively correlated with the number of other nodes connected. (**C**) GO terms of CQC anti-psoriasis candidate targets. (**D**) KEGG pathways of CQC anti-psoriasis candidate targets.

psoriasis were involved in many pathways, mainly including cell cycle, p53 signaling pathway, PI3K-Akt signaling pathway, IL-17 signaling pathway, AMPK signaling pathway, FOXO signaling pathway, PPAR signaling pathway, among others (Figure 4D).

Identification of CQC Anti-Psoriasis Core Targets by Multiple Machine Learning Algorithms

Modeling and cross-validation were performed using the Lasso regression algorithm (Figure 5A). Within the cross-validation analysis, the dotted line corresponds to lambda.min, signifying the optimal model fit (Figure 5B). At this juncture, the model identifies 13 distinct genes, specifically CCKBR, CCNB2, CFTR, AURKB, F3, NR3C2, CCNB1,

https://doi.org/10.2147/DDDT.S523836

HSD17B2, CDK5R1, CCNE1, CDK1, ARG1 and JAK3 (Figure 5C). To evaluate the performance of the model, the ROC curve was employed. The AUC value for the training set was 0.9699, whereas the AUC for the test set was 0.8958, which indicated the good accuracy of the model, as shown in Figure 5D.

In Random Forest, each decision tree had different selection of variables, and this training process was iteratively conducted to yield a total of 500 decision trees. The optimal number of trees was determined to be "ntree=175" at which point the error rate was minimized (Figure 5E), with the AUC in this model was 0.9793 in the training set, and 0.9333 in the test set (Figure 5F), signifying the usability and accuracy of the model. Figure 5G presents the ranking of candidate targets based on their Mean Decrease Gini index, the top 15 were selected as important genes, containing AKR1B10, AURKB, CA6, CCNB1, CCNB2, CCNE1, CDC25A, CDK1, HSD11B1, JAK3, MAPT, MMP1, NPY5R, PPARG, and TNNC1.

In SVM modeling, four kernel functions, including Linear Kernel, Polynomial Kernel, Radial Basis Kernel and Sigmoid Kernel, were substituted into the modeling respectively. The model prediction accuracy was shown in Figure 5H–K, with SVM_ linear training set AUC of 0.9352 and test set AUC of 0.9183, SVM_polynomial training set AUC of 0.9565 and test set AUC of 0.9286, SVM_radial training set AUC of 0.9674 and test set AUC of 0.9524, SVM_sigmoid training set AUC is 0.9051 and test set AUC is 0.8149. Subsequently, the kernel function was set to be Radial Basis Kernel for the establishment of the SVM model (Figure 5L), which identified 25 featured targets, including AKR1B10, ARG1, AURKA, AURKB, CCKBR, CCNB1, CCNB2, CCNE1, CDK1, CCNE2, CDC25A, and other associated targets.

Finally, upon integrating the feature targets derived from Lasso regression, Random Forest, SVM model, and hub-targets within the PPI network, a Venn diagram was drawn, as depicted in Figure 5M. Six CQC anti-psoriasis core targets (AURKB, CCNB1, CCNB2, CCNE1, CDK1, and JAK3) were obtained.

Verification of CQC Anti-Psoriasis Core Targets by ROC and Molecular Docking

The ROC curves demonstrated high diagnostic accuracy for AURKB (Figure 6A, AUC 0.925, 95% CI 0.871–0.980), CCNB1 (Figure 6B, AUC 0.983, 95% CI 0.953–1.000), CCNB2 (Figure 6C, AUC 0.974, 95% CI 0.942–1.000), CCNE1 (Figure 6D, AUC 0.994, 95% CI 0.983–1.000), CDK1 (Figure 6E, AUC 0.983, 95% CI 0.967–1.000), and JAK3 (Figure 6F, AUC 0.7872, 95% CI 0.805–0.940), which indicated that these core targets had great potential for psoriasis diagnosis. The gene expression levels of AURKB, CCNB1, CCNB2, CCNE1, CDK1 and JAK3 were significantly higher in the LS group compared to NL group (Figure 6G, $p<0.001$).

The molecular docking approach was employed to calculate the binding affinities between 29 main ingredients of CQC and these core targets. The protein-ligand complex structures of CCNB1 (PDB:2B9R), CCNE1 (PDB:1W98), AURKB (PDB:4AF3), CDK1 (PDB:4Y72), JAK3 (PDB:5TTS) were collected from RSCB PDB database, but the known structure of CCNB2 could not be retrieved. The plausible predicted structure of CCNB2 (AlphaFold:AF-O95067-F1) was retrieved from the AlphaFold database. As shown in Figure 6H, 67.2% of the binding energies were less than −7.0 kcal/mol. Among them, salvianolic acid A showed potential high binding affinity with AURKB, CCNB2, CCNE1, CDK1 and JAK3; Taxifolin 7-rhamnoside showed high binding affinity with AURKB, CCNB2, CDK1 and JAK3, and astilbin showed high binding affinity with AURKB and CDK1, and both engeletin and rosmarinic acid showed high binding affinity for CCNB1, all the complex conformations were shown in Figure 6I-K and Supplementary Figure 1–3.

Effect of CQC on IMQ-Induced Psoriasis-Like Symbol in Rats

The overall framework and chronology of the experimental design are outlined in Figure 7A. IMQ was spread on the skin of the depilated area on the back of rats for 7 consecutive days to induce the formation of psoriasis-like lesions. Figure 7B shows that during the modeling period from day 1–8, the IMQ-induced shaved dorsal skin areas of the four groups of modeling rats appeared distinctly red or crimson in color, with hypertrophied lesions, marked infiltration, and almost all the lesions were covered with flaky scales on the surface, which gradually developed into psoriasis-like skin lesions. While during the drug intervention period from day 8–15, psoriasis-like lesions exhibited varying degrees of alleviation in rats treated with MTX and different doses of CQC, with the most significant remission observed in the CQC_H group.

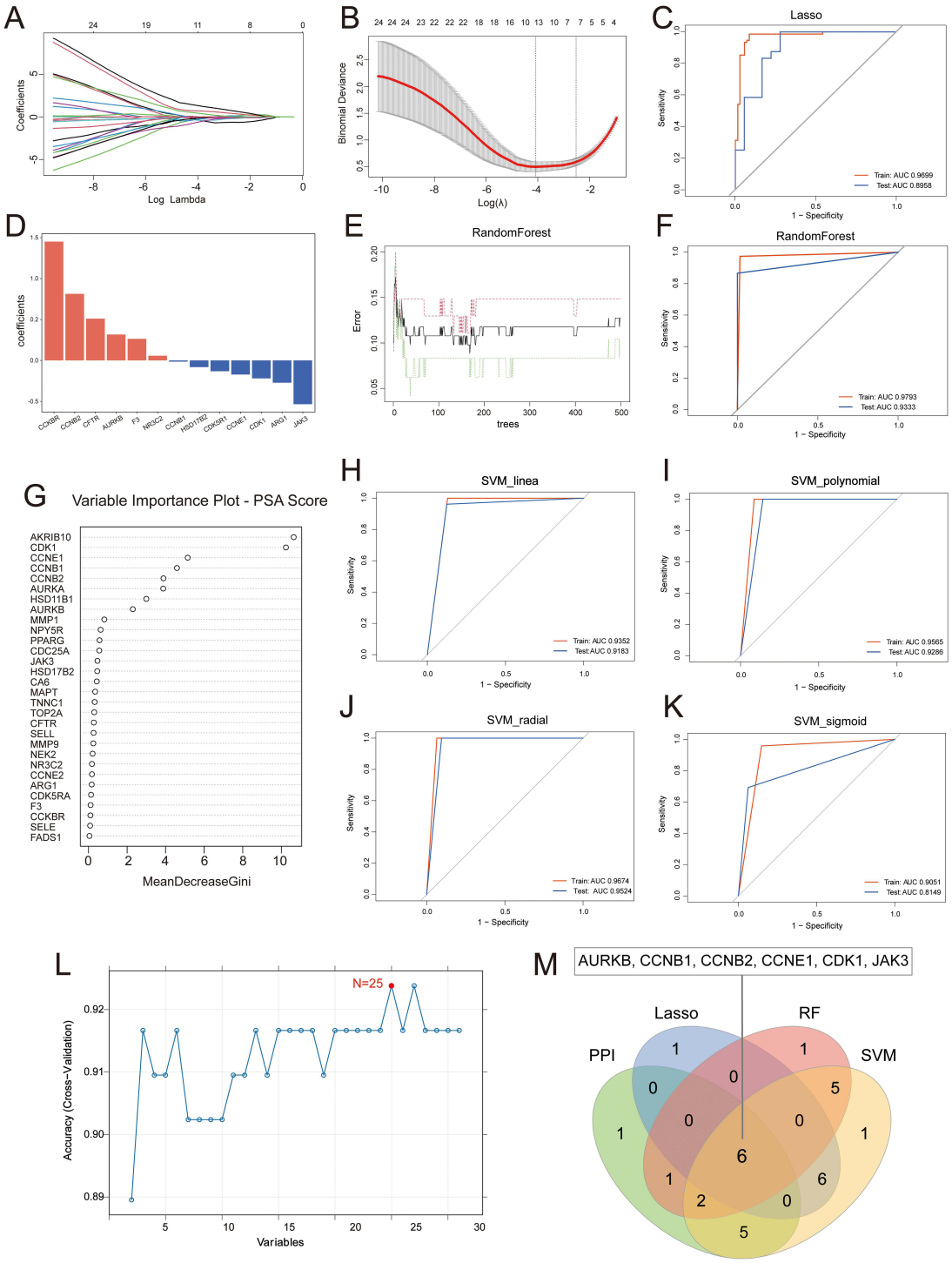

Figure 5 Identification of CQC anti-psoriasis core targets by using Machine learning. (**A**–**D**) LASSO regression algorithm screen characteristic targets from CQC anti-psoriasis candidate targets. (**A**) Path diagram of the regression coefficients for model fitting on the training set: the upper X-axis represents number of independent variables, the lower X-axis represents Log Lambda, each line represents one target gene, and Y-axis represents the regression coefficients corresponding to target genes. (**B**) Trend plot of the number of variable screenings corresponding to Log(λ) in the cross-validation model: the upper X-axis represents the number of independent variables, the lower X-axis represents the Log (λ) value corresponding to the value of λ, and Y-axis represents the mean square error. (**C**) ROC plots for the optimal Lasso regression model, training set in red, test set in blue. (**D**) Histogram of correlation coefficients of characterized genes screened by Lasso regression algorithm. (**E**–**G**) RandomForests screen characteristic key targets from CQC anti-psoriasis candidate targets. (**E**) Random forest model training effect diagram: X-axis represents the number of decision trees in the random forest model and Y-axis represents the proportion of misclassified samples. (**F**) ROC plots for the optimal RandomForests, training set in red, test set in blue. (**G**) Scatterplot of key targets in the optimal model of RandomForests: X-axis represents the Mean Decrease Gini of the key target, ie the importance of the key target to the model, and Y-axis represents the key target. (**H**–**L**) SVM screen characteristic targets from CQC anti-psoriasis candidate targets. ROC plots of SVM models constructed with linear kernel (**H**), polynomial kernel (**I**), radial kernel (**J**) and sigmoid kernel (**K**), training set in red, test set in blue. (**L**) Trend plot of variables screened number against sample prediction accuracy in the optimal SVM model: X-axis represents the number of feature variables, Y-axis represents the sample prediction accuracy corresponding to that number of samples, red dot represents the results of the optimal SVM model. (**M**) Intersection genes among PPI, LASSO regression algorithm, RandomForests and SVM, the CQC anti-psoriasis core targets.

https://doi.org/10.2147/DDDT.S523836

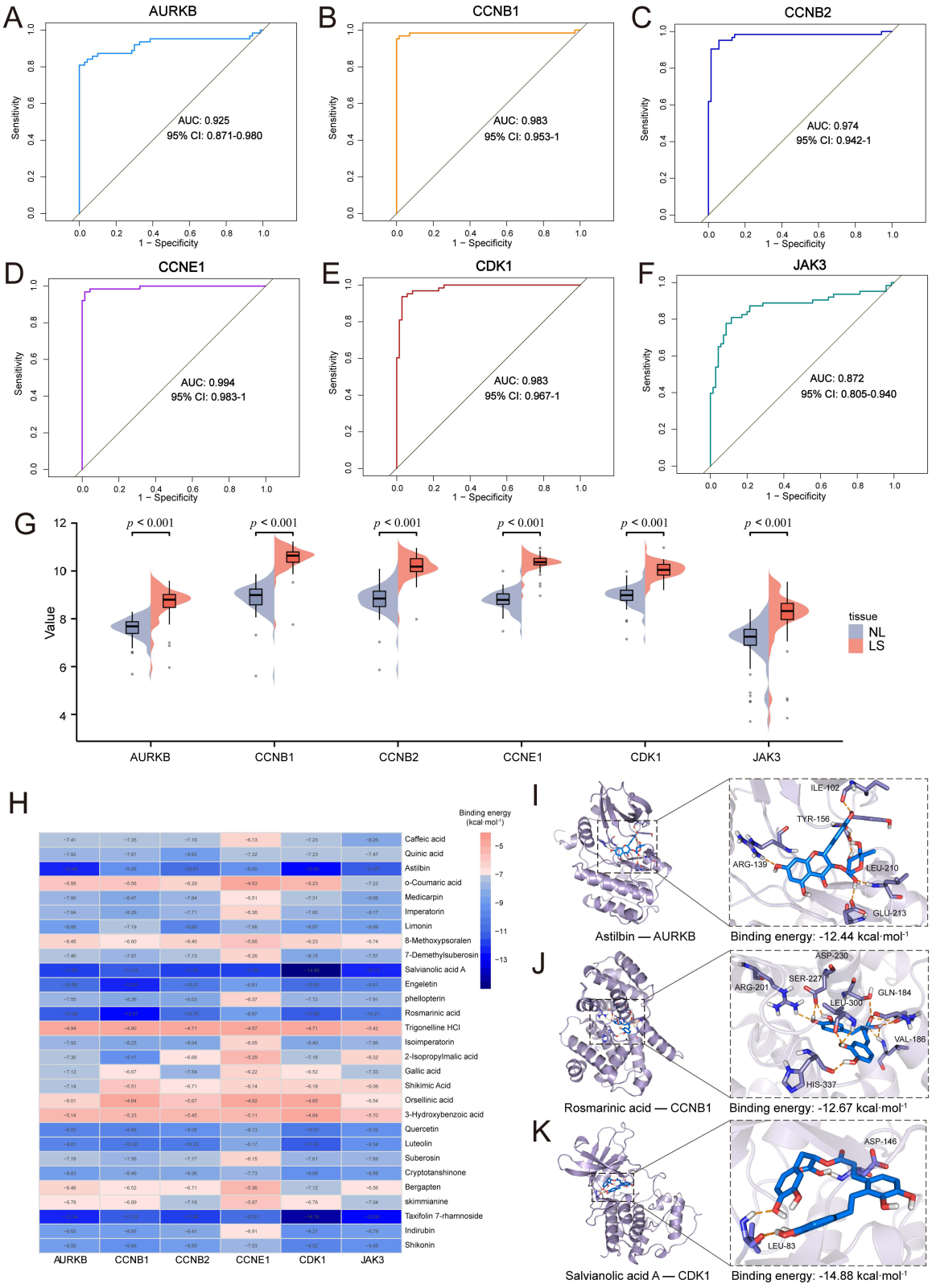

Figure 6 Validation of CQC anti-psoriasis core targets based on GSE201827 dataset. (**A-F**) ROC curves of AURKB (**A**), CCNB1 (**B**), CCNB2 (**C**), CCNE1 (**D**), CDK1 (**E**) and JAK3 (**F**). (**G**) Comparison of gene expression level of AURKB, CCNB1, CCNB2, CCNE1, CDK1, JAK3 between NL and LS groups. Data are represented as the mean ± SD (n: NL=70, LS=63) and t-tests were used for comparison of the significant differences. (**H**) Heatmap showed molecular docking results of core targets with CQC main ingredients. (**I**) The complex conformations charts for Astilbin with AURKB. (**J**) The complex conformations charts for Rosmarinic acid with CCNB1. (**K**) The complex conformations charts for Salvianolic acid A with CDK1.

 https://doi.org/10.2147/DDDT.S523836

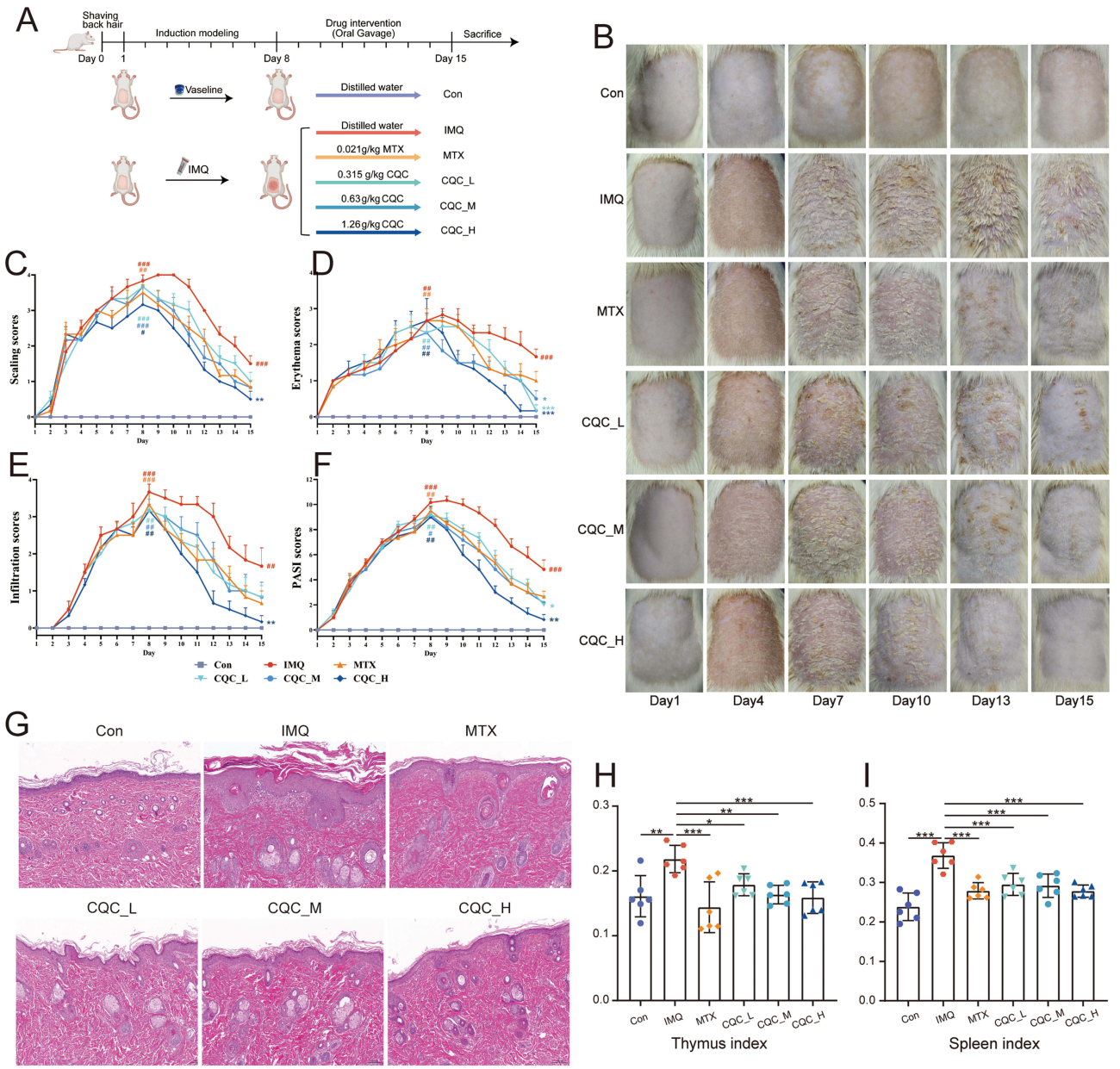

Figure 7 Relief of psoriasis-like skin lesions in rats induced by IMQ through CQC treatment. (**A**) Rats experimental design. (**B**) Changes in rats' back hair removal area in the six groups. (**C**–**F**) Trend graph of PASI scores in rats' back hair removal area in the six groups, including scaling (**C**), erythema (**D**), infiltration (**E**) and PASI scores (**F**). Data are represented as the mean ± SEM (n = 6), on the day 8, each group was compared with the Con group ($^{\#}p < 0.05$, $^{\#\#}p < 0.01$, $^{\#\#\#\#}p < 0.001$), on the day 15, the IMQ group was compared with the Con group ($^{\#}p < 0.05$, $^{\#\#}p < 0.01$, $^{\#\#\#\#}p < 0.001$), other groups was compared with the IMQ group ($^{*}p < 0.05$, $^{**}p < 0.01$, $^{***}p < 0.001$). (**G**) HE staining of rat back skin tissue under digital scanning laser microscope at 100× magnification. Effect of CQC on spleen index (**H**) and thymus index (**I**) in six groups of rats, data are represented as the mean ± SD, and each group was compared with the IMQ group. (n = 6, $^{*}p < 0.05$, $^{**}p < 0.01$, $^{***}p < 0.001$).

In the PASI assessment (Figure 7C-F), the scaling, erythema, infiltration and PASI scores exhibited a gradual increase across all modeling groups of rats during the day 1-8 modelling period, which induced by IMQ. Subsequently, during the drug intervention period from day 8–15, these scores decreased gradually to varying degrees, with the most significant reduction observed in the CQC_H group. HE staining (Figure 7G) analysis indicated that the skin lesions induced by IMQ presented with classic pathological traits of psoriasis, encompassing hyperkeratosis and parakeratosis, with Munro micro-abscess, and disappearance of the granular layer, thickening of the stratum spinosum, dilated capillaries in the dermis, and massive infiltration of inflammatory factors in epidermis and dermis. However, the IMQ-induced psoriasis-like symptoms were significantly improved with MTX and different doses of CQC, with normalization of keratinization,

https://doi.org/10.2147/DDDT.S523836

absence of Munro micro-abscess, thinning of the stratum spinosum, and reduction of inflammatory infiltrates in epidermis and dermis.

As shown in Figure 7H and I, the spleen and thymic index were increased in the IMQ group, whereas the reduction was evident following MTX administration and treatment with varying dosages of CQC. Notably, within CQC treated, a correlation was observed between the administered dose and the degree of decrease in the spleen index of the rats, and similar trend was observed for the thymus index.

Regulation of Core Gene Expression Levels in Skin Tissues of Psoriasis-Like Rats by CQC

In the qRT-PCR results (Figure 8), the mRNA expression levels of AURKB, CCNB1, CCNB2, CCNE1, CDK1 and JAK3 were significantly up-regulated in the IMQ group compared with the Con group, which was consistent with the changes in the expression of core targets in the GSE201827 dataset (Figure 6G). Compared to the IMQ group, different doses of CQC significantly down-regulated all core target genes expression, but MTX had no significant effect on AURKB and CDK1 expression.

ELISA detected the protein expression levels of core targets, as shown in Figure 9. Compared to the Con group, the expressions of AURKB, CCNB1, CCNB2, CCNE1 and CDK1 were significantly up-regulated in the IMQ group, but there was no significant change in JAK3 expression. Different doses of CQC and MTX significantly down-regulated the expression of all core targets compared with the IMQ group.

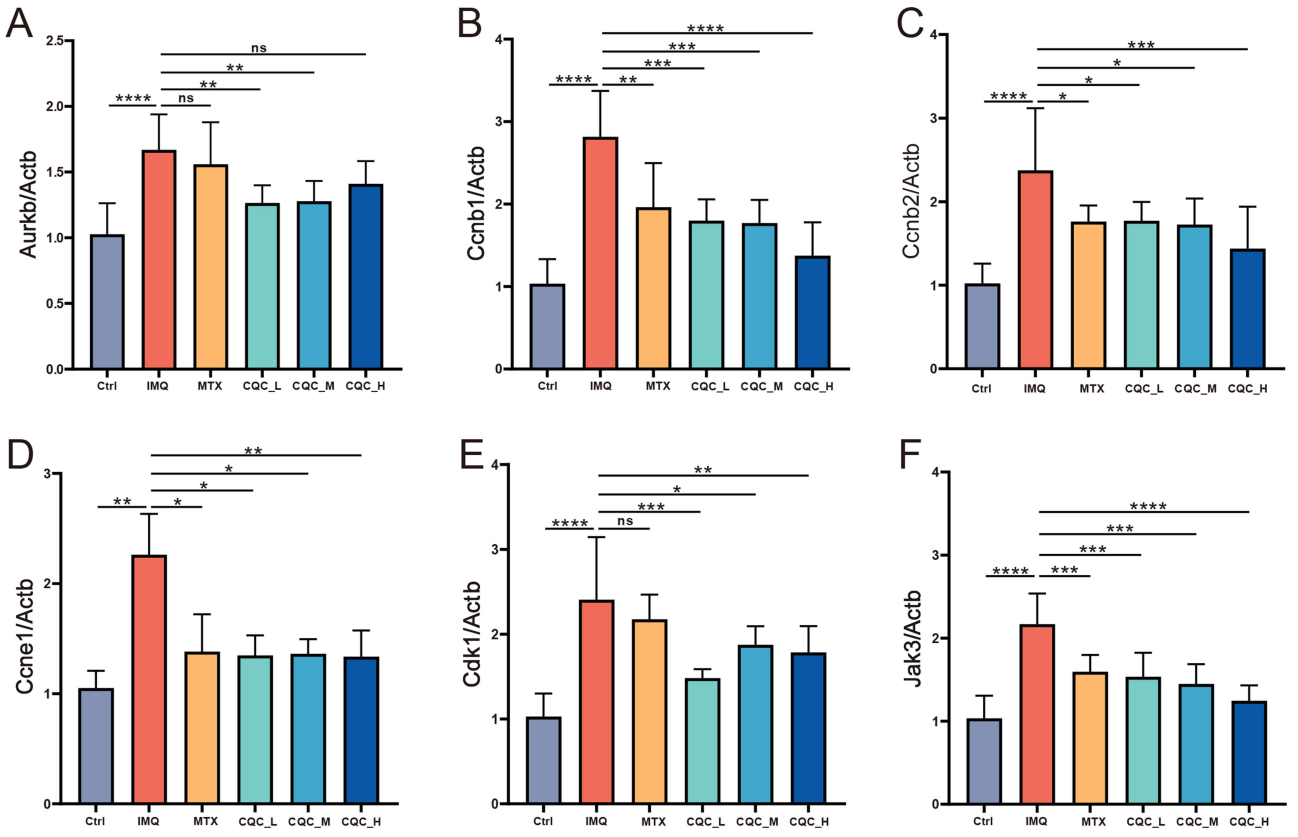

Figure 8 Down-regulation in the mRNA levels of core targets during CQC intervention in psoriasis-like rats. Effects of CQC on the mRNA expression levels of AURKB (**A**), CCNB1 (**B**), CCNB2 (**C**), CCNE1 (**D**), CDK1 (**E**) and JAK3 (**F**) in the skin tissues of six groups of rats. Data are represented as the mean ± SD, and each group was compared with the IMQ group. (n = 6, *$p < 0.05$, **$p < 0.01$, ***$p < 0.001$ and ****$p < 0.0001$).

 https://doi.org/10.2147/DDDT.S523836

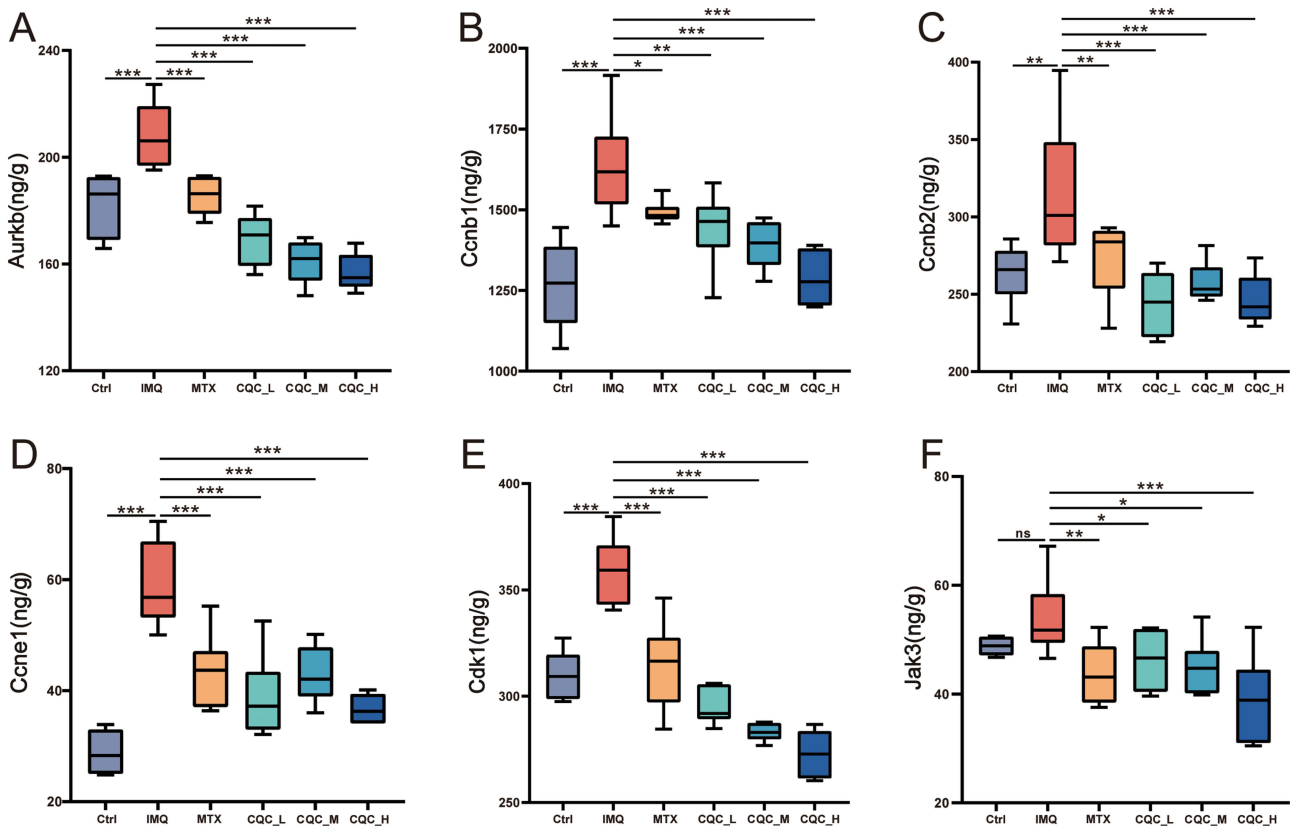

Figure 9 Down-regulation in the protein levels of core targets during CQC intervention in psoriasis-like rats. Effects of CQC on the protein expression levels of AURKB (**A**), CCNB1 (**B**), CCNB2 (**C**), CCNE1 (**D**), CDK1 (**E**) and JAK3 (**F**) in the skin tissues of six groups of rats. Data are represented as the mean ± SD, and each group was compared with the IMQ group. (n = 6, *$p < 0.05$, **$p < 0.01$, and ***$p < 0.001$.

Discussion

Psoriasis is a multifactorial condition with an intricate etiology, with its pathogenesis remain unclear. Despite the availability of treatments in modern medicine, their effectiveness is limited by factors such as drug resistance and immune predisposition. In contrast, TCM exhibits noteworthy benefits in the treatment of psoriasis, demonstrating multi-targets, multi-pathways while posing low side effects. Among them, CQC, as a widely used TCM preparation in clinical practice, has been proved to offer significant efficacy in psoriasis, alleviating effectively symptoms and enhancing immune function in patients, but the underlying molecular mechanisms remain unclear. Therefore, further exploration of its molecular mechanisms is crucial for clinical utilization and modernization of TCM.

In this study, psoriasis-associated multi-omics data were first analyzed to construct the psoriasis pathogenic pathway network. Within this network, the pathogenesis of psoriasis was found to involve multiple genes such as IL-17, CCNB1, CCNB2, CXCL1, CXCL2, and CXCL8, mediating Chemokine signaling pathway, cell cycle, PI3K-Akt signaling pathway, IL-17 signaling pathway and others (Figure 2F). Our group has validated the therapeutic potential of Traditional Chinese Medicine (TCM) in targeting the PI3K/AKT signaling pathway, offering a viable approach to managing psoriasis.[28] Moreover, several evidence highlighted the IL-17 signaling pathway's pivotal role in the disease's etiology and management. In this pathway, substances released from damaged keratinocytes can activate macrophages and dendritic cells to produce inflammatory factors IL-17 and TNF-α.[6,7] The concerted action of these cytokines not only induces the expression of antimicrobial defensins and cytokines but also chemokines, such as CXCL1, CXCL2, and CXCL8, which exacerbate psoriasis progression by mediating neutrophil infiltration in tissues through Chemokine signaling pathways.[29] Additionally, cell cycle-related genes such as CCNB1 and CCNB2 are found to serve as significant biomarkers in the etiology of psoriasis, suggesting that the cell cycle may play an important role.[30] In summary, the construction of the psoriasis pathogenic pathway network has provided profound insights into the interplay of key

https://doi.org/10.2147/DDDT.S523836

signaling pathways and the complex mechanisms of genes associated with psoriasis. This comprehensive understanding offers new avenues for innovative treatment strategies in the field of psoriasis management.

Utilizing UPLC-MS/MS technology, a total of 29 principal constituents of CQC were identified, encompassing a variety of compounds such as rosmarinic acid, caffeic acid, astilbin, salvianolic acid A, quercetin, isoimperatorin, shikonin, cryptotanshinone, limonin and engeletin (Figure 3A, B and Table 2). Our group has verified that rosmarinic acid can modulate the JAK2/STAT3 signaling pathway and suppress the IL-23/Th17 axis, alleviating psoriasis-like lesions in psoriasis-like rat models induced by IMQ.[31] Additionally, in the inflammatory state of HaCaT cells induced by LPS, rosmarinic acid, caffeic acid, and astilbin have been shown to not only inhibit cell proliferation but also effectively modulate inflammation levels.[28] Literature investigations have demonstrated that salvianolic acid A,[32] quercetin,[33] isoimperatorin,[34] shikonin,[35] cryptotanshinone,[36] limonin and engeletin[37] can effectively alleviate psoriasis symptoms by modulating inflammatory factors or inflammation-related signaling pathways through different molecular mechanisms. Given these findings, these ingredients may be the pharmacodynamic constituents of CQC in the treatment of psoriasis, considering as the potential main ingredients for further experimental investigation.

Next, systems pharmacology was performed to identify the interactions between the main ingredients of CQC and their related target genes, obtaining 31 candidate targets in the psoriasis pathogenic pathway network targeted by the main ingredients of CQC (Figure 4A). In the enrichment results, the regulation of cyclin-dependent protein serine/threonine kinase activity, and the regulation of cyclin-dependent protein kinase activity were significantly enriched in GO analysis, which indicated that these biological processes may be associated with CQC anti-psoriasis (Figure 4C). Abnormal proliferation and differentiation of keratinocytes within the epidermis constitute a pivotal factor in the pathogenesis of psoriasis, and the cell cycle plays a fundamental role in regulating the proliferative capacity of keratinocytes, contributing significantly to the pathogenesis of psoriasis.[38] Furthermore, the expression of p53 serves to facilitate DNA repair, arrest the cell cycle, and promote excessive proliferation of keratinocytes,[39,40] and the up-regulation of p53 expression can be observed in severe psoriasis lesions.[41] The analysis of KEGG pathway revealed that the cell cycle along with its upstream pathway, p53 signaling pathway, PI3K-Akt signaling pathway, were all significantly enriched, revealing their crucial roles in the molecular mechanism of CQC anti-psoriasis (Figure 4D).

The core targets of CQC anti-psoriasis (AURKB, CCNB1, CCNB2, CCNE1, CDK1 and JAK3) were screened using three machine learning algorithms, Lasso regression, Random Forest and SVM, and PPI analysis, for further modeling in the GSE201827 dataset (Figures 4B and 5A–M). AURKB, a serine/threonine protein kinase, is involved in the regulation of chromosome and cytoplasmic segregation during mitosis, and its elevated expression in the skin of psoriasis patients may promote skin cell mitosis, contributing to the disease's pathogenesis.[42] Similarly, CCNB1, which controls the G2/M transition of the cell cycle, can further promote mitotic activity when forming a complex with CDK1.[39] CCNB1 and CCNB2 have been correlated with the expression of cytokines such as IL-17A and IL-22, serving as biomarkers in psoriasis.[30] Additionally, miR-26a-5p can suppress the expression of genes associated with the IL-23/IL-17A axis, interfering with the CDC6/CCNE1 axis, and inhibiting the proliferation of psoriasis-like keratinocytes in vitro and in vivo.[43] Elevated CDK1 expression in psoriatic lesions and its up-regulation in HaCaT cells stimulated by IL-22 indicate its role in the disease's pathogenesis.[44] Drugs targeting cell cycle regulators, such as CDK inhibitors (eg, Palbociclib[45]), are being explored for their potential to reduce keratinocyte proliferation in psoriasis. Our identification of CDK1 and related cyclins (CCNB1, CCNB2, CCNE1) as targets suggests a similar mechanism of action, where inhibiting these proteins could slow down the hyperproliferative state of keratinocytes. And JAK3 has emerged as a potential target for the treatment of psoriasis, with its inhibitors being utilized in clinical practice.[46] JAK inhibitors (eg, Tofacitinib) are already in clinical use for various inflammatory and autoimmune diseases, including psoriasis. These drugs work by inhibiting the JAK-STAT pathway, thereby reducing the inflammatory response. Our finding that JAK3 is a potential target for CQC indicates a similar therapeutic strategy, focusing on modulating immune signaling to alleviate psoriasis symptoms.[47] These results revealed the vital role played by the core targets in the underlying pathophysiology of psoriasis. Molecular docking verified the binding affinities of 26 main ingredients of CQC with the core targets (Figure 6H), among which salvianolic acid A, taxifolin 7-rhamnoside, astilbin, engeletin, and rosmarinic acid exhibited high binding affinities with multiple core targets (Figure 6I–K and Supplementary Figure 1–3), further suggesting that these ingredients of CQC may target the core targets to exert therapeutic effects on psoriasis.

In animal experiments, the therapeutic efficacy of CQC on psoriasis-like rats was successfully verified following the induction of psoriasis-like lesions in the rats through IMQ. Observed alterations in the dorsal lesions of the rats revealed a notable reduction in scaling, erythema and infiltration of the dorsal skin in psoriasis-like rats treated with CQC, and the pathologic changes were also significantly improved (Figure 7B-G). Compared with the IMQ group, the spleen index and thymus index of psoriasis-like rats treated with CQC were significantly reduced, approaching the levels observed in the Con group. The results were similar to those of MTX treatment, further validating the therapeutic potential of CQC in the treatment of psoriasis-like conditions (Figure 7H and I). Importantly, even at the low dosage, CQC has demonstrated promising therapeutic effects on the psoriasis-like rats, suggesting a potential for effective treatment with smaller dosage. The qRT-PCR analysis was conducted to examine mRNA expression levels of core targets in rat skin tissues, and the results showed that the expression of core targets (AURKB, CCNB1, CCNB2, CCNE1, CDK1, and JAK3) in the model group showed significant up-regulation compared to the blank group, which was consistent with the gene expression trends obtained from the analysis in the GSE201827 dataset. However, the mRNA expression levels of these core targets were significantly down-regulated after CQC intervention (Figure 8). Consistent results were also observed in the protein expression levels detected by ELISA (Figure 9). These experimental results fully demonstrated that CQC not only effectively alleviated psoriasis-like skin lesions in rats, but also down-regulated the mRNA and protein expression levels of core targets, exerting the therapeutic effect on psoriasis. The findings underscore the importance of CQC as a potential therapeutic agent, for further unraveling the pathogenesis of psoriasis and for the broader clinical application of CQC.

In summary, our study identifies key targets (AURKB, CCNB1, CCNB2, CCNE1, CDK1, JAK3) involved in cell cycle and immune response pathways, which are dysregulated in psoriasis. These findings align with the broader context of TCM use, particularly polyherbal formulas like CQC, which are characterized by their good therapeutic effects and minimal side effects.[45,48] Our results support the potential of CQC to modulate multiple pathways simultaneously, thereby providing a comprehensive therapeutic effect. This is consistent with previous studies demonstrating enhanced treatment efficacy when combining TCM with conventional therapies, such as Chinese herbal medicine bath therapy[49,50] or oral TCM with Narrowband ultraviolet B (NB-UVB) therapy.[51] However, we acknowledge limitations such as the acute nature of the IMQ model, the need for high-quality datasets for machine learning, the complex composition of CQC, and the lack of cellular and in vitro validations. Future work will address these limitations by exploring chronic psoriasis models, integrating more experimental data, optimizing machine learning approaches, and conducting cellular and in vitro experiments to validate our findings.

Conclusion

In this study, we innovatively applied the combined strategy of multi-omics analysis, systems pharmacology, machine learning, molecular docking, and experimental validation to explore the molecular mechanisms underlying the therapeutic effects of CQC on psoriasis. The psoriasis pathogenic pathway network had been constructed, and 29 main ingredients of CQC were detected simultaneously. These ingredients would interact with 31 candidate targets in the psoriasis pathway network. Further analysis revealed that CQC may exert its pharmacological effects by modulating the activity of cell cycle-related proteins, via mechanisms that involve cell cycle, PI3K-Akt signaling pathway, and IL-17 signaling pathway. The application of three machine learning algorithms has identified six core targets of CQC's anti-psoriasis: AURKB, CCNB1, CCNB2, CCNE1, CDK1, and JAK3. The results of molecular docking revealed the high binding affinity of CQC ingredients, such as salvianolic acid A, astilbin, and rosmarinic acid, towards these core targets. Animal experiment subsequently verified the therapeutic efficacy of CQC anti-psoriasis, along with its significant modulation of core targets at both the mRNA and protein levels. Therefore, the findings confirmed that CQC may exert its therapeutic effects on psoriasis by targeting multiple targets within the pathogenic pathway network, including AURKB, CCNB1, CCNB2, CCNE1, CDK1, and JAK3, through various ingredients like salvianolic acid A, astilbin and rosmarinic acid, and mediates multiple signaling pathways.

Moving forward, we plan to further investigate the active ingredients of CQC and elucidate its specific mechanism of action through in vitro experiments. This approach will help us gain a deeper understanding of the molecular mechanism of action of CQC in the treatment of psoriasis.

Abbreviations

CQC, Compound Qingdai Capsules; UPLC-MS/MS, Ultra performance liquid chromatography/tandem mass spectrometry; SVM, Support Vector Machine; qRT-PCR, quantitative real-time reverse transcription polymerase chain reaction; ELISA, Enzyme linked immunosorbent assay; DEGs, Differentially expressed genes; DEMs, Differentially expressed microRNAs; AURKB, Aurora kinase B; CCNB1, Cyclin B1; CCNB2, Cyclin B2; CCNE1, Cyclin E1; CDK1, Cyclin dependent kinase 1; JAK3, Janus kinase 3; IMQ, Imiquimod; TCM, Traditional Chinese Medicine; GEO, Gene Expression Omnibus; KEGG, Kyoto encyclopedia of genes and genomes; NL, non-lesional skin; LS, lesional skin; PCA, principal component analysis; PPI, Protein-protein interaction; MCC, Maximal Clique Centrality; GO, Gene ontology; ROC, receiver operating characteristic; AUC, the area under the curve; MTX, Methotrexate; PASI, Psoriasis area severity index; HE, Hematoxylin-eosin staining; ACTB, beta-actin.

Ethics Approval

The animal experiments were strictly implemented following the Guidelines of the National Institutes of Health on Animal Care and Ethics and approved by the Animal Ethics Committee of Guangzhou University of Chinese Medicine (Approval Number: 202207006008).

GEO database is a publicly accessible repository, and used in this study were obtained from patients who had provided informed consent, and the data were anonymized to protect patient privacy. According to item 1 and 2 of Article 32 of the Measures for Ethical Review of Life Science and Medical Research involving Human Subjects (issued on February 18, 2023, in China), ethical review may be waived for studies that: (i) Utilize legally obtained public data, or data generated through observation without interfering with public behavior; (ii) Use anonymized information data for research purposes. Thus, the Ethics Committee of the First Affiliated Hospital of Guangzhou University of Chinese Medicine reviewing and waiving the need for ethical approval for the study.

Data Sharing Statement

The data used to support the findings of this study are available from the corresponding author upon request.

Acknowledgments

This work was supported by National Natural Science Foundation of China (grant no.81904198).

Author Contributions

All authors made a significant contribution to the work reported, whether that is in the conception, study design, execution, acquisition of data, analysis and interpretation, or in all these areas; took part in drafting, revising, or critically reviewing the article; gave final approval of the version to be published; have agreed on the journal to which the article has been submitted; and agree to be accountable for all aspects of the work.

Disclosure

The authors report no conflicts of interest in this work.

References

1. Eichenfield LF, Tarabar S, Forman S, et al. Efficacy and safety of PF-07038124 in patients with atopic dermatitis and plaque psoriasis: a randomized clinical trial. *JAMA dermatol*. 2024;160(2):156–163. doi:10.1001/jamadermatol.2023.4990
2. Singh A, Easwari TS. Recent advances in psoriasis therapy: trends and future prospects. *Current Drug Targets*. 2021;22(15):1760–1771. doi:10.2174/1389450122666210118103455
3. Griffiths CEM, Armstrong AW, Gudjonsson JE, Barker J. Psoriasis. *Lancet*. 2021;397(10281):1301–1315. doi:10.1016/S0140-6736(20)32549-6
4. Liu L, Lin NX, Yu YT, et al. Epidemiology of mental health comorbidity in patients with psoriasis: an analysis of trends from 1986 to 2019. *Psychiatry Res*. 2023;321:115078. doi:10.1016/j.psychres.2023.115078
5. Liu S, He M, Jiang J, et al. Triggers for the onset and recurrence of psoriasis: a review and update. *Cell commun signal*. 2024;22(1):108. doi:10.1186/s12964-023-01381-0

6. Kamata M, Tada Y. Dendritic cells and macrophages in the pathogenesis of psoriasis. *Front Immunol*. 2022;13:941071. doi:10.3389/fimmu.2022.941071
7. Vičić M, Kaštelan M, Brajac I, Sotošek V, Massari LP. Current concepts of psoriasis immunopathogenesis. *Int J Mol Sci*. 2021;22(21):11574. doi:10.3390/ijms222111574
8. Lee HJ, Kim M. Challenges and Future Trends in the Treatment of Psoriasis. *Int J Mol Sci*. 2023;24(17):13313. doi:10.3390/ijms241713313
9. Zheng W, Li, G, Liu Q, Wang H, Xu M, Ma H. Effect of compound qingdai capsule on cytokines secreted by hacat cells under micro environment of psoriasis. *Chin J Dermatovenereol*. 2021;35(03):261–265.
10. Shi G, An, Y, Zhou Y. Effect of compound qingdai capsule on th1/th2 shift in patients with psoriasis vulgaris. *World Chin Med*. 2022;17(19):2776–2780.
11. Committee on Psoriasis CSoD. Guideline for the diagnosis and treatment of psoriasis in China (2023 edition). *Chin Jl of Dermatol*. 2023;56(7):573–625.
12. Yang X, Wu D, Hou X, et al. Evaluation on clinical application of compound qingdai capsules. *Eval Anal Drug-Use Hospitals China*. 2022;22(07):871–875+881.
13. Deng J, Leijten E, Nordkamp MO, et al. Multi-omics integration reveals a core network involved in host defence and hyperkeratinization in psoriasis. *Clin transl med*. 2022;12(12):e976. doi:10.1002/ctm2.976
14. Lv S, Wang Q, Zhang X, et al. Mechanisms of multi-omics and network pharmacology to explain traditional Chinese medicine for vascular cognitive impairment: a narrative review. *Phytomedicine*. 2024;123:155231. doi:10.1016/j.phymed.2023.155231
15. Schulte-Sasse R, Budach S, Hnisz D, Marsico A. Integration of multiomics data with graph convolutional networks to identify new cancer genes and their associated molecular mechanisms. *Nature Mach Intell*. 2021;3(6):513–526. doi:10.1038/s42256-021-00325-y
16. Sharifi-Noghabi H, Zolotareva O, Collins CC, Ester M. MOLI: multi-omics late integration with deep neural networks for drug response prediction. *Bioinformatics*. 2019;35(14):i501–i509. doi:10.1093/bioinformatics/btz318
17. Xie G, Dong C, Kong Y, Zhong JF, Li M, Wang K. Group lasso regularized deep learning for cancer prognosis from multi-omics and clinical features. *Genes*. 2019;10(3):240. doi:10.3390/genes10030240
18. Chen H, He Y. Machine learning approaches in traditional Chinese medicine: a systematic review. *Am J Chin Med*. 2022;50(1):91–131. doi:10.1142/S0192415X22500045
19. Solvin Å, Chawla K, Olsen LC, et al. MicroRNA profiling of psoriatic skin identifies 11 miRNAs associated with disease severity. *Exp dermatol*. 2022;31(4):535–547. doi:10.1111/exd.14497
20. Blauvelt A, Pariser DM, Tyring S, et al. Psoriasis improvements and inflammatory biomarker normalization with secukinumab: the randomized ObePso-S study. *J Dermatological Sci*. 2023;109(1):12–21. doi:10.1016/j.jdermsci.2023.01.003
21. Gallo K, Goede A, Preissner R, Gohlke BO. SuperPred 3.0: drug classification and target prediction-a machine learning approach. *Nucleic Acids Res*. 2022;50(W1):W726–w731. doi:10.1093/nar/gkac297
22. Henke DM, Renwick A, Zoeller JR, et al. Bio-primed machine learning to enhance discovery of relevant biomarkers. *NPJ Precision Oncol*. 2025;9(1):39. doi:10.1038/s41698-025-00825-9
23. Salazar RM, Duryea JD, Leone AO, et al. Random forest modeling of acute toxicity in anal cancer: effects of peritoneal cavity contouring approaches on model performance. *Int J Radiat Oncol Biol Phys*. 2024;118(2):554–564.
24. Dong C, Yang N, Zhao R, et al. SVM-based model combining patients' reported outcomes and lymphocyte phenotypes of depression in systemic lupus erythematosus. *Biomolecules*. 2023;13(5). doi:10.3390/biom13050723.
25. Varadi M, Bertoni D, Magana P, et al. AlphaFold protein structure database in 2024: providing structure coverage for over 214 million protein sequences. *Nucleic Acids Res*. 2024;52(D1):D368–d375. doi:10.1093/nar/gkad1011
26. Schön MP, Manzke V, Erpenbeck L. Animal models of psoriasis-highlights and drawbacks. *J Allergy Clin Immunol*. 2021;147(2):439–455.
27. Shahine Y, El-Aal SAA, Reda AM, et al. Diosmin nanocrystal gel alleviates imiquimod-induced psoriasis in rats via modulating TLR7,8/NF-κB/micro RNA-31, AKT/mTOR/P70S6K milieu, and Tregs/Th17 balance. *Inflammopharmacology*. 2023;31(3):1341–1359. doi:10.1007/s10787-023-01198-w
28. Xie M, Zhang M, Qiao Y, et al. Molecular mechanism of PSORI-CM01 for psoriasis by regulating the inflammatory cytokines network. *J Ethnopharmacol*. 2024;318(Pt A):116935. doi:10.1016/j.jep.2023.116935
29. Moos S, Mohebiany AN, Waisman A, Kurschus FC. Imiquimod-induced psoriasis in mice depends on the IL-17 signaling of keratinocytes. *J invest dermatol*. 2019;139(5):1110–1117. doi:10.1016/j.jid.2019.01.006
30. Li AH, Chen YQ, Chen YQ, Song Y, Li D. CCNB1 and CCNB2 involvement in the pathogenesis of psoriasis: a bioinformatics study. *J Int Med Res*. 2022;50(8):3000605221117138. doi:10.1177/03000605221117138
31. Zhang M, Li N, Cai R, et al. Rosmarinic acid protects mice from imiquimod induced psoriasis-like skin lesions by inhibiting the IL-23/Th17 axis via regulating Jak2/Stat3 signaling pathway. *Phytother Res*. 2021;35(8):4526–4537. doi:10.1002/ptr.7155
32. Zhang QL, Jiang RH, Li XM, et al. Inhibition of poly(I:C)-induced inflammation by salvianolic acid A in skin keratinocytes. *Annals dermatol*. 2019;31(3):279–285. doi:10.5021/ad.2019.31.3.279
33. Zhang Y, Gong S, Liu L, et al. Cyclodextrin-coordinated liposome-in-gel for transcutaneous quercetin delivery for psoriasis treatment. *ACS Appl Mater Interfaces*. 2023;15(34):40228–40240. doi:10.1021/acsami.3c07582
34. Tsai YF, Chen CY, Lin IW, et al. Imperatorin alleviates psoriasiform dermatitis by blocking neutrophil respiratory burst, adhesion, and chemotaxis through selective phosphodiesterase 4 inhibition. *Antioxid Redox Signaling*. 2021;35(11):885–903. doi:10.1089/ars.2019.7835
35. Tao T, Chen Y, Lai B, et al. Shikonin combined with methotrexate regulate macrophage polarization to treat psoriasis. *Bioengineered*. 2022;13(4):11146–11155. doi:10.1080/21655979.2022.2062090
36. Tang L, He S, Wang X, et al. Cryptotanshinone reduces psoriatic epidermal hyperplasia via inhibiting the activation of STAT3. *Exp dermatol*. 2018;27(3):268–275. doi:10.1111/exd.13511
37. Chen L, Chen H, Lu Y, et al. Decoding active components in a formulation of multiple herbs for treatment of psoriasis based on three cell lines fishing and liquid chromatography-mass spectrometry analysis. *J Pharmaceut Biomed Anal*. 2020;186:113331. doi:10.1016/j.jpba.2020.113331
38. Huang YZ, Zheng YX, Zhou Y, et al. OAS1, OAS2, and OAS3 contribute to epidermal keratinocyte proliferation by regulating cell cycle and augmenting ifn-1–induced jak1–signal transducer and activator of transcription 1 phosphorylation in psoriasis. *J invest dermatol*. 2022;142(10):2635–2645.e2639. doi:10.1016/j.jid.2022.02.018

39. Dorai S, Alex Anand D. Differentially expressed cell cycle genes and STAT1/3-driven multiple cancer entanglement in psoriasis, coupled with other comorbidities. *Cells*. 2022;11(23):3867. doi:10.3390/cells11233867
40. Dadwal N, Amisha, Singh D, Singh A. Quality-by-design approach for investigating the efficacy of tacrolimus and hyaluronic acid-loaded ethosomal gel in dermal management of psoriasis: in vitro, ex vivo, and in vivo evaluation. *AAPS Pharm Sci Tech*. 2023;24(8):220. doi:10.1208/s12249-023-02678-6
41. Wang Q, Wang C, Zhao X, et al. MicroRNA-31 overexpression may aggravate the formation of psoriasis-like lesions by STAT3/p53 pathway. *Indian j dermatol*. 2021;66(6):598–603. doi:10.4103/ijd.ijd_10_21
42. Shah ET, Molloy C, Gough M, et al. Inhibition of Aurora B kinase (AURKB) enhances the effectiveness of 5-fluorouracil chemotherapy against colorectal cancer cells. *Br J Cancer*. 2024;130(7):1196–1205. doi:10.1038/s41416-024-02584-z
43. Li J, Pang D, Zhou L, Ouyang H, Tian Y, Yu H. Yu H. miR-26a-5p inhibits the proliferation of psoriasis-like keratinocytes in vitro and in vivo by dual interference with the CDC6/CCNE1 axis. *Aging*. 2024;16(5):4631–4653. doi:10.18632/aging.205618
44. Fang Y, C E, Wu S, Meng Z, Qin G, Wang R. Circ-IGF1R plays a significant role in psoriasis via regulation of a miR-194-5p/CDK1 axis. *Cytotechnology*. 2021;73(6):775–785. doi:10.1007/s10616-021-00496-x
45. Chen SH, Chen CH, Lin HC, Yeh SA, Hwang TL, Chen PJ. Drug repurposing of cyclin-dependent kinase inhibitors for neutrophilic acute respiratory distress syndrome and psoriasis. *J Adv Res*. 2024;2024:1.
46. Kumar N, Kuang L, Villa R, Kumar P, Mishra J. Mucosal epithelial jak kinases in health and diseases. *Mediators Inflammation*. 2021;2021:6618924. doi:10.1155/2021/6618924
47. Bachelez H, Griffiths CEM, Papp KA, et al. Tofacitinib efficacy, patient-reported outcomes and safety in patients with psoriasis and a medical history of psoriatic arthritis: pooled analysis of two Phase III studies. *J Eur Acad Dermatol Venereol*. 2024;38(7):e557–e561. doi:10.1111/jdv.19701
48. Gupta P, Kalvatala S, Joseph A, Panghal A, Santra S. Outline of therapeutic potential of different plants reported against psoriasis via in vitro, pre-clinical or clinical studies. *Phytother Res*. 2025;39(2):1139–1173. doi:10.1002/ptr.8405
49. Wang J, Zhang CS, Zhang AL, Changli Xue C, Lu C. Chinese herbal medicine bath therapy for psoriasis vulgaris using topical calcipotriol as the comparator: a systematic review with meta-analysis and association rule analysis. *J Ethnopharmacol*. 2024;330:118166. doi:10.1016/j.jep.2024.118166
50. Wang J, Zhang CS, Zhang AL, Chen H, Xue CC, Lu C. Adding Chinese herbal medicine bath therapy to conventional therapies for psoriasis vulgaris: a systematic review with meta-analysis of randomised controlled trials. *Phytomedicine*. 2024;128:155381. doi:10.1016/j.phymed.2024.155381
51. Jo HG, Kim H, Baek E, Seo J, Lee D. Efficacy and safety of orally administered east asian herbal medicine combined with narrowband ultraviolet b against psoriasis: a bayesian network meta-analysis and network analysis. *Nutrients*. 2024;16(16). doi:10.3390/nu16162690

Drug Design, Development and Therapy

Dovepress
Taylor & Francis Group

Publish your work in this journal

Drug Design, Development and Therapy is an international, peer-reviewed open-access journal that spans the spectrum of drug design and development through to clinical applications. Clinical outcomes, patient safety, and programs for the development and effective, safe, and sustained use of medicines are a feature of the journal, which has also been accepted for indexing on PubMed Central. The manuscript management system is completely online and includes a very quick and fair peer-review system, which is all easy to use. Visit http://www.dovepress.com/testimonials.php to read real quotes from published authors.

Submit your manuscript here: https://www.dovepress.com/drug-design-development-and-therapy-journal